INORGANIC CHEMISTRY

FRONTIERS

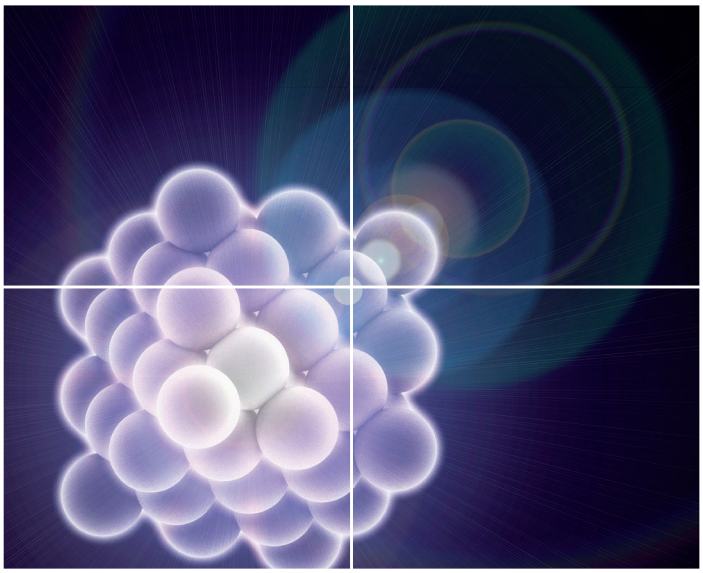

Accepted Manuscript

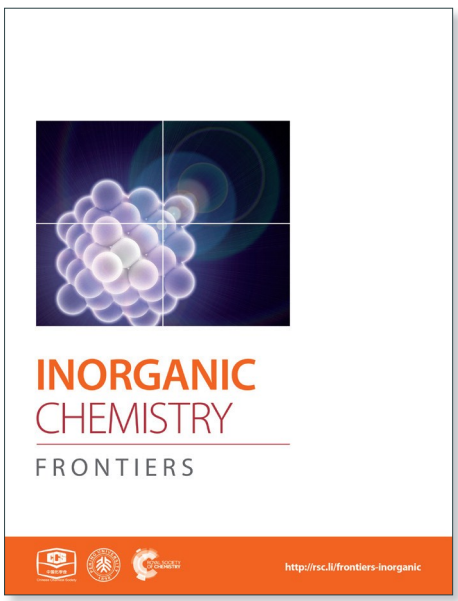

This is an *Accepted Manuscript*, which has been through the Royal Society of Chemistry peer review process and has been accepted for publication.

Accepted Manuscripts are published online shortly after acceptance, before technical editing, formatting and proof reading. Using this free service, authors can make their results available to the community, in citable form, before we publish the edited article. We will replace this *Accepted Manuscript* with the edited and formatted *Advance Article* as soon as it is available.

You can find more information about *Accepted Manuscripts* in the **Information for Authors**.

Please note that technical editing may introduce minor changes to the text and/or graphics, which may alter content. The journal's standard **Terms & Conditions** and the **Ethical guidelines** still apply. In no event shall the Royal Society of Chemistry be held responsible for any errors or omissions in this *Accepted Manuscript* or any consequences arising from the use of any information it contains.

Journal Name

ARTICLE

Microstructure construction and composition modification of CeO_2 macrospheres with superior performance

Received 00th January 20xx,
Accepted 00th January 20xx

DOI: 10.1039/x0xx00000x

www.rsc.org/

Xiaodan Yang,[a,†] Shuaiyu Jiang,[a,†] Jun Chen,[a] Xianran Xing,[a] Lianzhou Wang,[b] and Ranbo Yu,[a,b,*]

Macro/nano-composite CeO_2 spheres with variable diameters of 30-300μm assembled from nanoparticles of 5-8nm were synthesized through the calcination of the well assembled spherical $Ce(COOH)_3$ precursor. The controlled hydrolysis of the DMF is the key factor for both the crystallization of $Ce(COOH)_3$ and the formation of its macrospheres. These hierarchical CeO_2 macrospheres possess pretty high specific surface areas of up to ~190 m^2/g and show an excellent ability to remove Cr(VI) from aqueous solution. Moreover, when substituted with Bi(III), the oxygen storage capacity (OSC) of these CeO_2 spheres could be improved sharply to 3243.75 μmol[O]/g. With the easy-to-manipulate macroscale spherical morphology, these materials are easily recycled. This synthesis opens a promising route for high performance metal oxides.

Introduction

In recent years, hierarchical structures with special morphology and novel properties attracted more and more research interests.[1-4] As hierarchical assemblies of nanoscale building blocks may have characteristics of both the nanostructure and the microstructure, and the ordered three dimensional (3D) nanostructures for the development of nanodevice with high performance. Moreover, the assembled nanostructures may be more environmental friendly than the nanosized material regarding the problem of the nanosecurity. Many methods have been used to prepare hierarchical 3D structures of various functional materials, including the thermal reduction process,[5] thermal oxidation process,[6] oriented aggregation,[7] self-assembly of building blocks through hydrophobic interactions,[8] and template-assisted synthesis.[9]

CeO_2 possesses remarkable properties due to its abundant oxygen vacancy defects, high oxygen storage capacity and ability to relatively easily shuttle between III and IV oxidation states. It has been extensively studied and employed in many applications, such as active component of three-way catalysts (TWC),[10-12] photocatalysts for water oxidation,[13] oxygen ion conductors in solid oxide fuel cells, [14-16] and ultraviolet (UV) blocking materials in UV shielding.[17] Because of the improvements in the redox properties, specific surface area to volume ratio, and transport properties with respect to condensed bulk materials, nanostructured and porous CeO_2 or CeO_2-based compounds has attracted special attention. [18-28] Recently, various nano-sized CeO_2 have been obtained. However, improvement of surface area were not obvious. On the other hand, synthesis of mesoporous CeO_2 could give surface area up to 200 m^2/g,[21] but the random products morphology was not desirable for further application. To build up hierarchical 3D nanostructures would be a promising route to CeO_2 with larger specific surface area and desirable morphologies. Mesoporous CeO_2 microspheres with uniform flowerlike morphologies were synthesized by using glucose and acrylamide as templates, but its surface area is only 92.2m^2/g.[27] We explored new routes to build up 3D multi-shell hollow structures.[13,28] Although these structures show good performance as catalysts, whose lower specific surface area of ~95 m^2/g is still not desirable. Therefore a facial route for the growth of CeO_2 with both high surface area and uniform morphology is still in need.

In this work, an in situ structure directing formation strategy is adopted in the synthesis of hierarchically macrospherical $Ce(COOH)_3$ precursors by controlling the hydrolysis of DMF. The macrospherical $Ce(COOH)_3$ precursors could be easily transformed into perfect CeO_2 macrospheres upon calcinations. The obtained CeO_2 macrospheres possessed high surface area and showed an excellent ability to remove Cr (VI) from aqueous solution. Moreover, when doped with Bi (III), the oxygen storage capacity (OSC) of the CeO_2 increased significantly with no obvious decrease of surface area.

Experimental

All the chemicals were purchased from Beijing Chemical Reagent Company and used without further purification.

[a] Department of Physical Chemistry, University of Science and Technology Beijing, Beijing 100083, PR China.
[b] Nanomaterials Centre, School of Chemical Engineering and AIBN, The University of Queensland, St. Lucia, Brisbane, QLD, 4072, Australia
* Corresponding author. E-mail: ranboyu@ustb.edu.cn, Tel. +86-10-62332525, Fax. +86-10-62332525.
† These authors contributed equally to this work.

Electronic Supplementary Information (ESI) available: TG-DSC isotherm, crystal structure, the N_2 adsorption-desorption isotherms, FE-SEM image, SEM-EDAX. See DOI: 10.1039/x0xx00000x

Preparation of CeO_2 macrospheres and hollow macrospheres

The synthesis was performed in a system of $(NH_4)_2Ce(NO_3)_6$-EtOH-DMF, similar to the method we have reported in previous work.[29] In a typical experiment, ammonium cerium nitrate was dissolved into grain alcohol under magnetic stirring for at least 30 min, followed by addition of DMF to form a transparent orange solution, the molar ratio of $(NH_4)_2Ce(NO_3)_6$-EtOH-DMF was 1: 86: 72. The solution was aged under hydrothermal conditions at 100-150 $^{\circ}C$ for 4-6 days in a Teflon-lined stainless steel autoclave. After washed thoroughly followed by drying at 60 $^{\circ}C$, the macrospherical $Ce(COOH)_3$ precursor was obtained. In order to adjusting the precursor formation, HAc aqueous (wt 36%) was used as the reaction media instead of EtOH, and the hollow macrospheres of $Ce(COOH)_3$ precursor were synthesized by using. These two kinds of spherical precursors were further calcined at 350$^{\circ}C$ for 3 h using a temperature programmed muffle furnace with a heating rate of 1 $^{\circ}C \cdot min^{-1}$, the porous CeO_2 macrospheres were finally obtained.

Characterization

The phases and purity of the products were examined by X-ray powder diffraction (XRD) performed on M21XVHF22 X-ray diffractometer (Japan) with Cu Kα radiation (λ = 1.5418 Å). The morphology of the products was observed by a field emission scanning electron microscope (LEO1530) and a high resolution transmission electron microscopy (HRTEM, Philips CM-30, 3000 kV). The nitrogen adsorption-desorption isotherms at 77 K were measured using a Quantachorme Instruments AUTOSOR8-1C Powders Adsorption Analyzer.

The OSC and water treatment test

For the water treatment experiment, $K_2Cr_2O_7$ was used as the source of Cr(VI), the pH values of the solutions were adjusted using HCl or NaOH. Solutions containing different concentrations of Cr(VI) were prepared and adjusted to pH = 3. Then, 0.05 g of the adsorbent sample was added to 25 mL of the above solution under stirring. After a specified time, the solid and liquid were separated and Atomic Absorption Spectrometry (AA-6800) was used to measure the chromium concentration in the remaining solutions. The adsorption isotherm was obtained by varying the initial Cr(VI) concentrations and stirring for 5 h at room temperature (20 °C).

The OSC measurements were carried out at 500 °C. The measurements were carried out in a flow reactor system equipped with solenoid valves for rapid introduction of (4%) CO + (1%) Ar + He or (2%) O_2 + (1%)Ar + He pluses. Typically, 30 mg powders were loaded into a 1.0 cm id. quartz tube reactor and a total gas flow rate of 300 $cm^3 \cdot min^{-1}$ was employed. The signals of the outlet gas were detected by an on-line quadrupole mass spectrometer (Omnistar 200). Prior to CO step measurements, the sample was heated in (2%) O_2+ (1%)Ar + He at 773K for at least 20 min. The sample was further purged in pure He for 30 min to remove oxygen from the system and then exposed to (4%) CO + (1%) Ar + He. The accumulated amount of CO_2 per gram of catalyst was monitored as a function of time.

Results and discussion

Two kinds of the macrospherical precursors were hydrothermally synthesized by adjusting the synthesis conditions. Their phase purity and crystal structure of the precursors were examined by XRD. The XRD patterns of the two samples (Figure 1a) shows that they are both pure and of the same phase. All the peaks could be readily indexed as the rhombohedral cerium formate (ICSD No.069333, space group: R3m). To get the final CeO_2 products, the precursors would undergo the calcination. The calcination temperature was determined according to the thermogravimetric (TG) analysis of the precursor (see the Supporting Information Figure S1). A total weight loss of 33.4% was observed in the temperature range of 180-310°C due to the pyrolysis of the organic species in the precursor. So the CeO_2 could be obtained from heating cerium formate precursor at temperature higher than 350 °C, which could be confirmed by the XRD pattern of the calcined product (Figure 1b). The patterns of calcined products can be indexed as a pure face-centered cubic phase of CeO_2 (PDF No.:43-1002, space group: Fm3m).

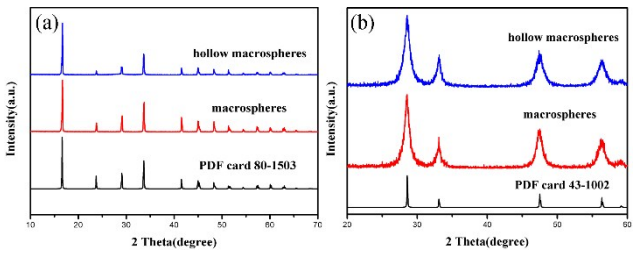

Figure. 1 XRD patterns of (a) the macrospherical precursors and (b) calcined products.

The morphology and structure of the precursors and final products were characterized by using the field emission scanning electron microscope (FE-SEM) and the high-resolution transmission electron microscope (HRTEM). It can be observed that by adjusting the hydrothermal synthesis conditions, general and hollow macrospheres of the precursor and the CeO_2 could be obtained. Figure 2a shows most of the as-synthesized $Ce(COOH)_3$ precursor possesses uniform spherical morphology with the average size of 300 μm, upon calcination at 350°C these $Ce(COOH)_3$ transformed into CeO_2 spheres without any obvious shrinkage or destroy of the spherical morphologies (Figure 2b). From the HRTEM image it can be seen that these CeO_2 macrospheres are composed of many crystalline CeO_2 nanoparticles with an average diameter of 5-8nm. The hollow CeO_2 macrospheres could also be obtained by calcining the as-prepared $Ce(COOH)_3$ hollow macrospheres (Figure 2c, d).

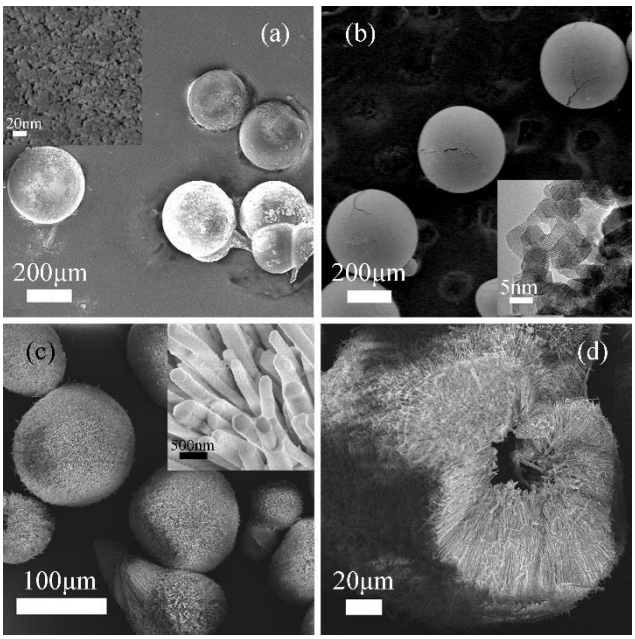

Figure. 2 FE-SEM image, (a) $Ce(COOH)_3$ macrospheres precursor, inset is the surface of the macrospheres, (b) CeO_2 macrospheres, inset is the HRTEM image of the CeO_2 macrospheres, (c) $Ce(COOH)_3$ hollow macrospheres precursor, inset is the surface of the hollow macrospheres (12 h), (d) CeO_2 hollow macrospheres, cut with the blade showing the image of section.

In this synthesis, the DMF plays a crucial role in the formation of the microspheres. In the acid system, DMF might hydrolyze into formic acid and dimethylamine as following Equation:

$$C_3H_7ON + H_2O \xrightarrow{H^+} C_2H_7N + HCOOH \quad (1)$$

The formic acid would react with cerium sources to form $Ce(COOH)_3$, and dimethylamine might act as structure-directing agent to help the microspheres assembly. To determine the detailed effect of DMF, the following comparison processes have been tested. When the formic acid was used instead of DMF, under the same reaction conditions, only a cluster of cerium formate just like Irish diamond could be obtained. And when the formic acid and dimethylamine were used together, microrods of cerium formate with rough-and-tumble diameters could be synthesized but no macrospheres assembly could be observed (Figure S3). Obviously, both the hydrolysis process and products of DMF are dominant for the formation of $Ce(COOH)_3$ macrospheres. Apparently, to realize the morphology control of $Ce(COOH)_3$ precursor it is necessary to control the hydrolysis rate of DMF. Because acid will enhance the hydrolysis of DMF, the acetic acid and ethanol were used as the solvents, respectively. Under different hydrolysis rate of DMF, the formation of hollow and general hierarchical $Ce(COOH)_3$ macrospheres was achieved, respectively (Figure 2).

To gain insight into the formation process of cerium formate macrospheres, time-dependent experiments were performed. Products were collected at different stages from the reaction mixture once the precipitate had begun to appear in solution, and their morphologies were subjected to FE-SEM investigation. However, for the general $Ce(COOH)_3$ macrospheres, it is difficult to capture the product images at different reaction stages, because the formation of the macrospheres is too fast after the $Ce(COOH)_3$ nucleation. For the hollow $Ce(COOH)_3$ macrospheres, the first sample was taken immediately after the formation of precipitate when reacted for 90 min, the powder were comprised with broom-like microrods (Figure S4a). In this phase, the cerium formate formed a pyramid first, and then the top end was splited into nanorods (Figure S4a). After 15 min, the nanorods with diameters of about 40nm and lengths up to 6μm began to self-assemble into microspheres. Although the nanorods grew thicker, the diameter of the microspheres kept still. Hollow microspheres formed over the following 1.5 h (Figure S4b), which grew up evidently bigger in the further 6 hours. From these four obvious morphology evolutionary stages a possible formation process is proposed as Figure 3. At first, the hydrolysis of the DMF led to the nucleation of $Ce(COOH)_3$, which is further grow in to one-dimensional nanorods. With the increase of the reaction time the concentration of organic amine increased, which would probably result in the increase of surface energy of the $Ce(COOH)_3$ nanorods. To decrease the surface energy the bundles formed after treatment for 1.5 h. These bundles gradually organized into microspheres when the reaction time was extended to 3 h, which is possible related to the structure-directing effect of the organic amine. In the associations through carboxylic acid and amino groups, hydrogen bonding patterns may direct structure formation in the solution, generating specific supramolecular crystal architectures held together by networks of H-bonds.[30, 31] At the end of the reaction (12h), a hollow macrosphere was observed.

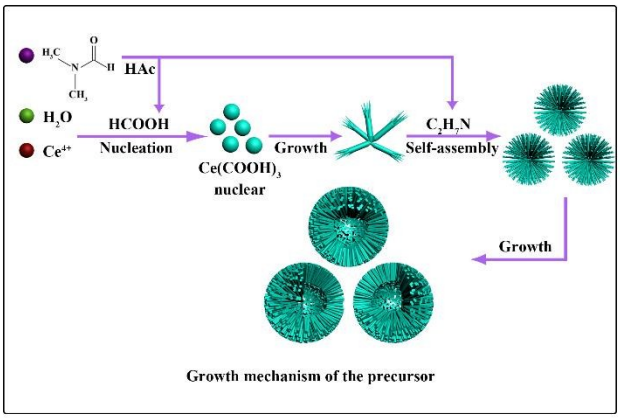

Figure. 3 Possible Formation Process for the macrospheres.

The N_2 adsorption-desorption isotherms of $Ce(COOH)_3$ and CeO_2 macrospheres are given in Supporting Information

(Figure S5-S8), respectively. These isotherms lie between type-I and type-IV. The pore size distribution curves are shown in the inset to their own adsorption-desorption isotherm figures. The average pore diameters are showed in the supporting information. The distribution of the pore diameters is multistage. After calcination, the pore size distribution becomes widely. The BET surface areas of CeO_2 macrospheres and hollow macrospheres calculated from these isotherms are 185.1m^2/g and 154.7m^2/g, respectively.

Clean water, free of toxic chemicals and pathogens, is vital to the world's health, and is also a critical feedstock in a variety of key industries. Some nanostructured metal oxides showed higher capacities for toxic ions and organic pollutants removal from water than bulk material [32-34]. Moreover, as the size of these oxides was several to hundred micrometers, the solid/liquid separation would be fairly easy. With the high specific surface area and hierarchical porous structure, the capacity for Cr(VI) removal from aqueous solutions of the as-synthesized CeO_2 macrospheres was investigated. Chromium is considered as one of the primary highly toxic pollutants in water resources and its efficient removal from water is of great importance. Figure S9 shows that when 0.05 g of as-obtained CeO_2 was added to 25 mL of chromium solution with an initial concentration of 21.00 mg L^{-1} and adjusted to pH=3 at room temperature (20 °C), the adsorption capacity was measured as 7.9 mg Cr g^{-1}, and the adsorption rate could reach to 80%, especially, when the initial concentration of the chromium solution is 10 mg L^{-1}, the adsorption rate could achieve 97%. The Cr removal ability of the hierarchical CeO_2 macrospheres are much higher than that (adsorption rate: 65%) of the 3D flowerlike CeO_2 micro/nanocomposite structure.[33]

The total oxygen storage capacity (OSC) can express the maximum OSC and contains information about the overall reducibility of the solid. The OSC values of the as-synthesized CeO_2 macrospheres and hollow macrospheres were measured as 1471.43 and 1168.75 μmol[O]/g, respectively. For comparison, the OSC of the commercial cerium oxides with particle size of about 50nm and the BET specific surface area of 24.97 m^2/g has also been measured, and the corresponding OSC value of 611.61 μmol[O]/g was obtained, which is much lower than that of the as-synthesized CeO_2 macrospheres. The possible reason is the higher surface area of the as-synthesized CeO_2 macrospheres enhanced the oxygen storage capacity.

It is reported that when CeO_2 is doped with Bi(III), the OSC can be improved, due to the increase of the surface oxygen vacancies.[35] So in this work, further research about Bi(III) doped CeO_2 macrospheres are also explored. The XRD pattern of Bi/CeO_2 macrospheres (Figure 4a) indicates the face-centered cubic phase of CeO_2 has been maintained. The BET specific surface area of Bi/CeO_2 could reach at 192.7m^2/g(Figure S10). EDX analysis (Figure S11 and Table S1) shows that the amount of Bi(III) is 4%(atom%). The FE-SEM image (Figure 4b) shows the Bi/CeO_2 macrospheres are uniform and in good distribution. There is no obvious change of the spherical morphologies after Bi(III) was doped. In the Raman spectra (Figure 4c), peak shift and a shoulder at around 490 cm^{-1} can be observed after Bi(III) was doped. These proved that the Bi(III) might be incorporated into the structure of CeO_2. The OSC of the corresponding materials achieve much higher values, 3243.75 μmol[O]/g. The dynamic OSC comparison of the CeO_2 and the Bi/CeO_2 macrospheres (Figure 4d) at different temperatures in the range of 200°C-600°C indicated that the Bi doped sample show much better performance than pure CeO_2 macrospheres.

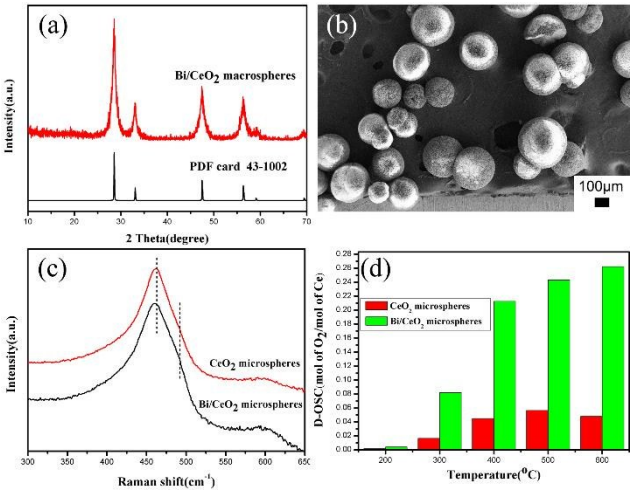

Figure. 4 Bi doped CeO_2 macrospheres: (a) XRD patterns, (b) FE-SEM image, and Raman spectra (c) and D-OSC (d) of CeO_2 and Bi/CeO_2 macrospheres.

Conclusions

In summary, a facile route has been developed to synthesize hierarchical CeO_2 macrospheres with high surface area and large pore volume. Controlled synthesis of $Ce(COOH)_3$ precursor macrospheres with variable sizes could be realized under the low-temperature hydrothermal conditions. DMF and its hydrolysis in the reaction system contribute to both the crystallization of $Ce(COOH)_3$ and the assembly of its macrospheres. With the high specific surface area and easy to control size, the final CeO_2 macrospheres proved to be both effective sorbents for water treatment and potential catalysts with high OSC value for redox reactions. Furthermore, Bi(III) doping will further improve their OSC dramatically, which make these materials the promising candidates for technical as catalyst, solid oxide fuel cells, and oxygen pump. Moreover, this easily repeated synthesis route could also be used in related materials preparation, and will open a new approach to functional materials with high specific surface area and performance.

Acknowledgements

This work was financially supported by National Natural Science Foundation of China (No. 21271021, 51472025) and

Program for Changjiang Scholars and Innovative Research Team in University (IRT 1207).

Notes and references

1 W. Shenton, D. Pum, U. B. Sleytr, S. Mann, *Nature* 1997,**389**,585.
2 R. P. Panmand, Y. A. Sethi, S. R. Kadam, M. S. Tamboli, L. K. Nikam, J. D. Ambekar, C. J. Park, B. B. Kale, *CrystEngComm*, 2015, **17**, 107.
3 L. Passoni, L. Criante, F. Fumagalli, F. Scotognella, G. Lanzani, F. Di Fonzo, *ACS nano*, 2014, **8** 12167.
4 Z. K. Zheng, W. Xie, Z. S. Lim, L. You, J. L. Wang, *Scientific reports*, 2014, **4**
5 Y. B. Li, Y. Bando, D. Golberg, *Appl. Phys. Lett. ,* 2003, **82**, 1962.
6 A. C. Chen, X. S. Peng, K. Koczkur, B. Miller, *Chem. Commun. ,* 2004, 1964.
7 B. Liu, H. C. Zeng, *J. Am. Chem. Soc. ,* 2004, **126**, 8124.
8 M. R. Molla, S. Ghosh, *Phys. Chem. Chem. Phys.*, 2014, **16**, 26672.
9 Z. Liu, Y. Yang, J. H. Mi, X. L. Tan, C. Lv, *International Journal of Hydrogen Energy*, 2013, **38** 4445.
10 E. Aneggi, C. de Leitenburg, G. Dolcetti, A. Trovarelli, *Catal. Today,* 2006, **114**, 40.
11 L. G. Appel, J. G. Eon, M. Schmal, *Phys. Status Solidi a,* 1997, **163**, 107.
12 A. Bruix, J. A. Rodriguez, P. J. Ramírez, S. D. Senanayake, J. Evans, J. B. Park, D. Stacchiola, P. Liu, J. Hrbek, F. Illas, *J. Am. Chem. Soc.* 2012, **134**, 8968.
13 J. Qi, K. Zhao, G. D. Li, Y. Gao, H. J. Zhao, R. B. Yu, Z. Y. Tang, *Nanoscale*, 2014, **6**, 4072.
14 Z. L. Zhan, S. A. Bamett, *Science*, 2005, **308**, 844.
15 H. J. Beie, A. Gnorich, *Sens. Actuators B,* 1991, **4**, 393.
16 P. Jasinski, T. Suzuki, H. U. Anderson, *Sens. Actuators B*, 2003, **95**, 73.
17 R. Si, Y. W. Zhang, L. P. You, C. H. Yan, *J. Phys. Chem. B,* 2006, **110***,* 5994.
18 A. Corma, P. Atienzar, H. Garcia, J. Y. Chane-Ching, *Nat. Mater.,* 2004, **3**, 394.
19 S. C. Laha, R. Ryoo, *Chem. Commun.,* 2003, 2138.
20 D. Terribile, A. Trovarelli, J. Llorca, C. de Leitenburg, Dolcetti, G. *J. Catal.* 1998, **178**, 299.
21 D. M. Lyons, K. M. Ryan, M. A. Morris, *J. Mater. Chem.,* 2002, **12**, 1207.
22 A. Bouchara, G. D. Soler-Illia, J. Y. Chane-Ching, C. Sanchez, *Chem. Commun.,* 2002, 1234.
23 S. Yang, L. Gao, *J. Am. Chem. Soc.,* 2006, **128**, 9330.
24 L. Yan, X. R. Xing, R. B. Yu, J. X. Deng, J. Chen, G. R. Liu, *Physical B: Condensed Matter*, 2007, **390**, 59.
25 L. Yan, R. B. Yu, J. Chen, X. R. Xing, *Cryst. Growth Des. ,* 2008, **8**, 1474.
26 R. B. Yu, L. Yan, P. Zheng, J. Chen, X. R. Xing, *J. Phys. Chem. C*, 2008, **112**, 19896.
27 C. W. Sun, J. Sun, G. L. Xiao, H. R. Zhang, X. P. Qiu, H. Li, L. Q. Chen, *J. Phys. Chem. B*, 2006,**110**,13445.
28 P. F. Xu, R. B. Yu, H. Ren, L. B. Zong, J. Chen, X. R. Xing, *Chem. Sci.*, 2014, **5**, 4221.
29 X. Yao, X. D. Yang, R. B. Yu, P. F. Xu, J. Chen, X. R. Xing, Materials Research Bulletin, 2015, 61, 22.
30 J. Zhang, S. J. Liu, J. Lin, H. S. Song, J. J. Luo, E. M. Elssfah, E. Ammar, Y. Huang, X. X. Ding, J. M. Gao, S. R. Qi, C. G. Tang, *J. Phys. Chem. B,* 2006, **110**, 14249.
31 J. M. Lehn, Supramolecular Chemistry Concepts and Perspectives, *Angewandte Chemie-English Edition*, 1995, **34**, 2563.
32 P. Li, D. E. Miser, S. Rabiei, R. T. Yadav, M. R. Hajaligol, *Appl. Catal. B,* 2003, **43**, 151.
33 R. C. Wu, J. H. Qu, Y. S. Chen, *Water Res.,* 2005, **39**, 630.
34 L. S. Zhong, J. S. Hu, A. M. Cao, Q. Liu, W. G. Song, L. J. Wan, *Chem. Mater*. 2007,**19**,1648.
35 N. Imanaka, T. Masui, K. Koyabu, K. Minami, T. Egawa, *adv. mater*. 2007,**19**,1608.